Modeling, Simulation, and Measurement of a Full-Scale, Integrated Energy Efficiency-Retrofit Prototype for Single-Family Attached Residences in Cold Climates

By Shayan Mirzabeigi, LEED Green Associate; Sameeraa Soltanian-Zadeh; Rui Zhang, PhD; Bess Krietemeyer, PhD; Zhenlei Liu, PhD; and Jianshun "Jensen" Zhang, PhD

This paper was presented at the 2024 IIBEC/OBEC BES.

INTRODUCTION

In the United States, buildings contribute to 38% of carbon dioxide (CO_2) emissions, consume 73% of total electricity, and account for 39% of total energy usage.[1] About 20% of that total energy is consumed by residential buildings. Residential buildings constructed before energy codes were established represent approximately 68% of all building stock in the United States,[2] and they often have significant air leakage and inadequate insulation. As a result, heating and cooling losses in these buildings can account for a substantial portion of utility bills. Deep energy retrofits that achieve significant reductions in energy used for space conditioning and producing domestic hot water are needed to enable conversion of heating to clean energy without exceeding the capability of existing electric grids, and for reducing energy bills of households in historically underserved communities.[3]

The building enclosure is one of the main targets in energy retrofit projects to reduce overall energy consumption and the environmental impact of buildings, especially in cold climates.[4,5] High-performance buildings incorporate a combination of tight building enclosures, mechanical ventilation, and energy-efficient components to ensure comfort, adequate airflow, and moisture control.[6] In this context, prefabricated panelized exterior insulated enclosure systems are emerging as a promising technology for retrofit solutions.[7,8] The project described herein focused on the design, development, and testing of

proof-of-concept prototypes for a replicable, cost-effective "one-stop shop" retrofit solution that addresses the need for innovation in integrated design, fabrication, and installation. The solution comprises a prefabricated modular exterior enclosure system that is compatible with a high-efficiency mechanical pod for heating, cooling, ventilation, and domestic hot water supplies.

The overall goal of this project was to develop a transformative solution for integrated whole-building energy efficiency retrofits of residences in cold or very cold climate regions; the first target was a solution for single-family attached residences with the potential of extending the approach to extend the approach to single-family detached homes and low-rise multifamily housing. The project team developed a novel highly insulated prefabricated modular exterior building enclosure retrofit wall system and enclosure-integrated HVAC system components that connect to a compatible and optimally sized modular mechanical pod to deliver heating, cooling, ventilation, and domestic hot water.

Reviewing similar approaches of exterior building enclosure retrofit wall systems,[9] there is a need to quantify the panel performance relative to insulating value and airtightness.[9] The primary research questions are: What is the impact of air leakage on the hygrothermal performance of a retrofitted panel system under varying pressure differentials? How do infiltration and exfiltration affect the hygrothermal performance? What is the effective R-value of the retrofitted panel system, including the effects of leakage and joints? Therefore, this study measured the influence of air leakage on hygrothermal performance of a full-scale integrated energy efficiency retrofit assembly, installed at Syracuse University's Building Envelope Systems Test (BEST) facility, under different pressure differentials, modeled the effects of both infiltration and exfiltration using Combined Heat, Air, Moisture and Pollutant Simulation for Building Envelope Systems (CHAMPS-BES).[10] It assessed the effective R-value of a retrofitted panel system, considering the effects of leakage and joints, and validated the results through the full-scale tests. In addition, an EnergyPlus model was developed.[11] This model was used to simulate the whole building energy savings potential (total thermal energy use intensity (EUI) reduction) of the retrofitted building prototype in comparison with a reference that represents existing conditions of the same type of buildings to assess the technical potential for energy-savings from all applicable buildings in the United States.

MATERIALS AND METHODS

This study evaluates the performance of an energy efficiency retrofit prototype using field measurements and modeling. The research was conducted at BEST facility, a state-of-the-art laboratory designed to simulate and measure the performance of building enclosure systems. The research involved monitoring hygrothermal conditions in March 2022. The collected data validated a model-based evaluation methodology using the CHAMPS-BES software. Notably, the testing of the mechanical pod was not within the scope of this paper. This section is divided into four subsections, including (1) BEST Lab Setup; (2) Descriptions of the measurements; (3) Effective R-value quantification; and (4) Modeling and simulation.

1. BEST Lab Setup:

The BEST Lab is a two-story building on the Syracuse University South campus, located at Syracuse, New York, that is a baseline residential building used for research and development related to building enclosure systems and energy performance. **Figure 1** shows an overview of the BEST facility (top left), lower corner section on the first floor used for testing (bottom) and the domain of interest for hygrothermal simulation (top right). The southeast corner room with two exterior walls exposing east and south was selected for the purpose of the full-scale prototype installation and testing of the integrated enclosure and mechanical retrofit system. In the design of the panel layout, the objective was to maintain the minimum number of panels and seams to maintain thermal performance while considering impacts on aesthetics and cost. The panel layout and structural attachment system for the BEST Lab full-scale prototype test were driven by the overall building dimensions, foundation, existing wall assembly, elevation, locations of windows and doors. Panels were prefabricated for the installation and field testing at the BEST facility. Six mid-scale prototypes, for the integrated building enclosure retrofit system, were designed and fabricated, and tested to represent varying panel types and connections, including: (1) Opaque panel with no seams; (2) Panel-to-panel with a horizontal seam; (3) Panel-to-panel with a vertical seam; (4) Panel-to-panel with a vertical and horizontal seam; (5) Panel-to-window; (6) Panel-to-HVAC penetration. Two separate chamber tests measured thermal resistance and airtightness of each mid-scale prototype.[12] Thermal resistance and airtightness testing of panels with vertical, horizontal, and cross-joint seams showed anticipated decreases in thermal resistance and increases in air leakage compared with the opaque panel. Air leakage was especially greater than expected, with significant air-leakage at the vertical and cross-joint seams. The difference of results across panel types demonstrated the importance of compression in a panel module assembly and attachment strategy. It also informed a revised gasket strategy. **Figure 1** shows a photo of the completed prototype on the BEST facility, with different panel types and seam conditions.

2. Descriptions of the measurements:

Type T thermocouples and heat flux sensors were used to measure the exterior and interior surface temperatures and heat fluxes on the interior surface, in order to calculate the effective thermal resistance of the whole assemblies and to validate the hydrothermal simulations. An interior test room was constructed to set up a realistic experiment. A total of 59 sensors were mounted to the south, east, north, and west walls of the test room. The sensor mounting
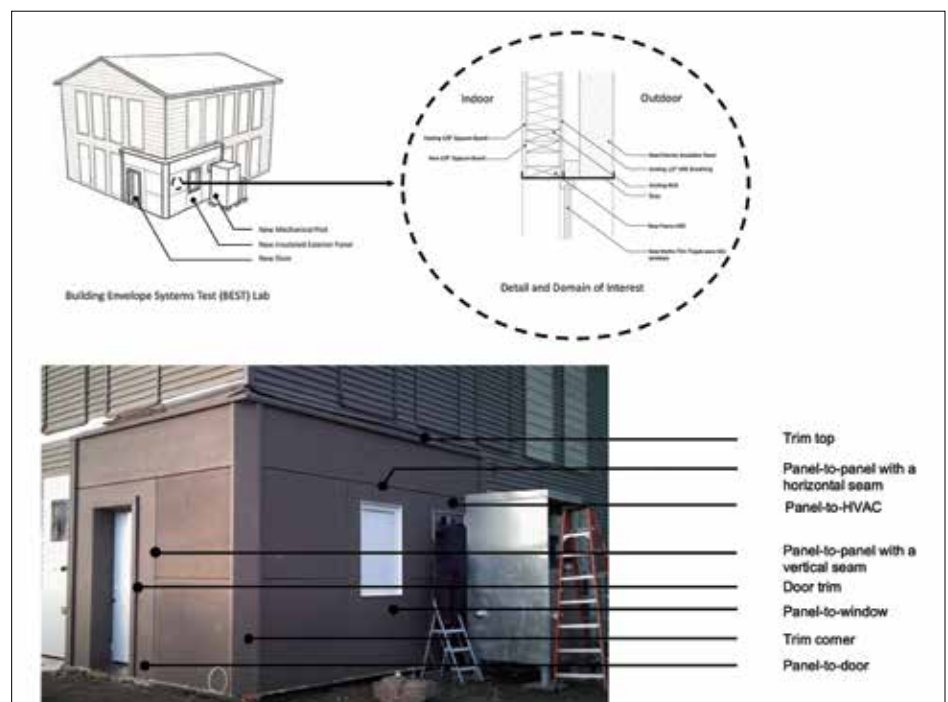

Figure 1. *Schematic of the case study (top), and the completed prototype with different panel types and seam conditions (bottom).*
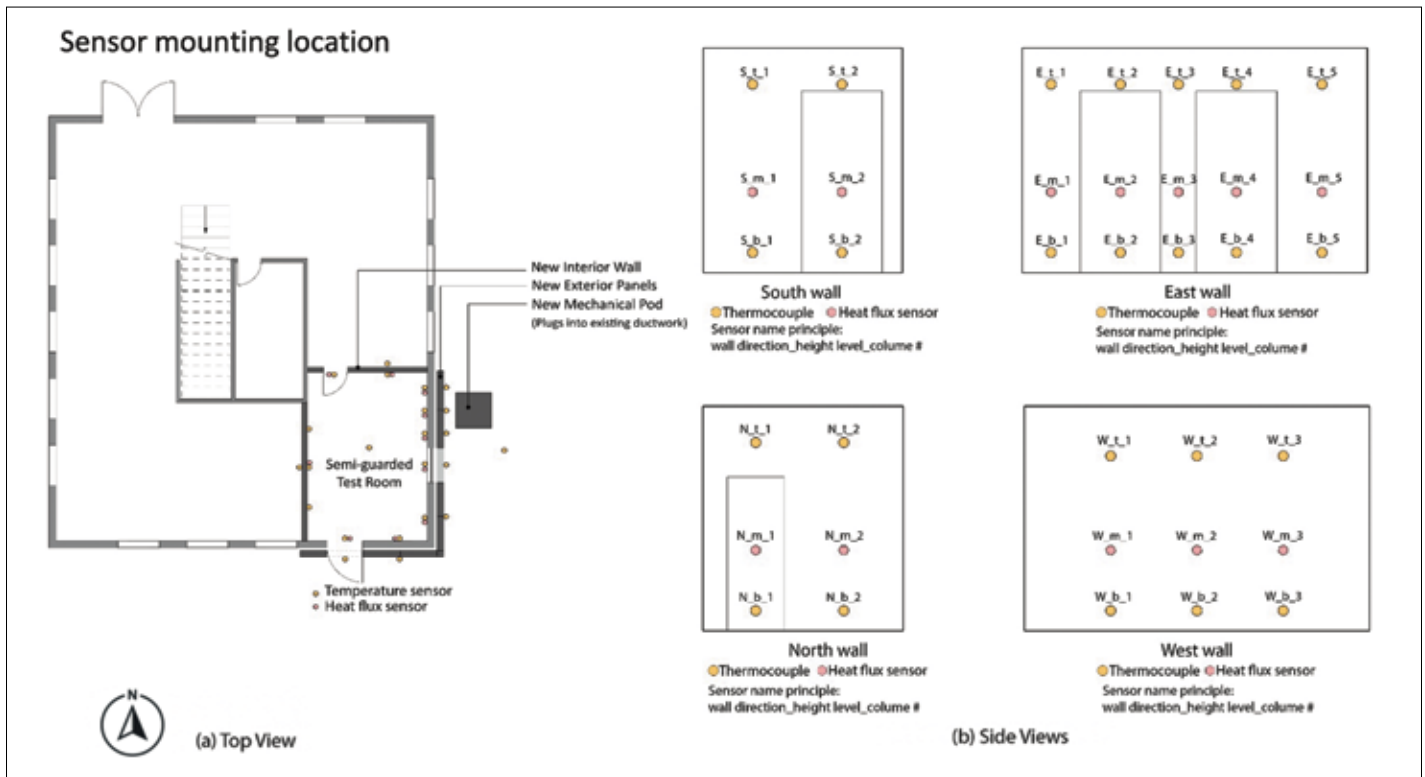
Figure 2. *Sensor-mounting locations.*

locations are shown in **Fig. 2.** They were selected to include different types of wall sections (plain walls, door, or penetration for the pod) and three vertical sections (top, middle, and bottom). The east wall contained 15 interior sensors, mounted in alignment with 15 exterior sensors. Each sensor on the east wall measured different panel conditions, for example, an opaque structural panel, a panel with an opening for a window, and a panel with an opening for mechanical component penetrations.

The south wall contained 6 interior sensors, mounted in alignment with 6 exterior sensors positioned at an opaque panel area and at an exterior door. The north internal partition wall contained 6 interior sensors located at an internal door and an internal wall. The west wall contained 9 interior sensors. Additional thermocouples were used to monitor the indoor and outdoor air temperatures. The data acquisition was built using a Campbell CR3000 datalogger with three multiplexers. The data collection interval was 10 minutes.

3. *R*-value quantification:

The effective thermal resistance was calculated at each sensor location from measured in-situ temperature difference among indoor, air gap, and outdoor environment and heat flux data by using summation technique over time. The estimation of the effective thermal resistance R_e is calculated by using summation technique as below.[13]

$$R_e = \frac{\sum_{k=1}^{M} \Delta T_k}{\sum_{k=1}^{M} q_k} \qquad (1)$$

where

R_e = thermal resistance, m²K/W (ft² °F h/BTU)

M = number of values of ΔT and q in the source data

ΔT = difference in temperature between the indoor surface and the air gap for the existing construction, *K; or* difference in temperature between the air gap and the outdoor environment for the retrofitting plane, *K*

k = counter for summation of timeseries data

q = heat flux, W/m² (BTU/h·ft²)

To determine the time to compute the estimated thermal resistance, the convergence factor CR_n was calculated using Eq. (2), where *n* is time units (12 hours).

$$CR_n = \frac{R_e(t) \quad R_e(t-n)}{R_e(t)} \qquad (2)$$

At the selected time, CR_n remains below 0.1 for at least three periods of length n. The variance of *R*-values $V(R_e)$ is used at least two more times to evaluate whether the thermal resistance

of the building component is acceptable or not. $V(R_e)$ is calculated as follows:

$$V(R_e) = [s(R_e)/\text{mean}(R_e)] \text{ x } (100\%) \qquad (3)$$

where $s(R_e)$ is calculated with (*N* – 1) degrees of freedom, and *N* is the number of values of (R_e) (*N* ≥ 3).

4. Modeling and simulations:

Advanced exterior enclosure retrofitting systems represent high thermal resistance. However, different insulation components are connected to each other using gaskets. Correspondingly, additional leakage around seams may affect the components' hygrothermal behavior. The main challenge of this problem lies in modeling of airflow through joints, cavities, and cracks, where determining the exact leakage path is difficult. Assuming a small path in the junction area with an airflow due to a pressure differential, heat and moisture transfer can take place between the flowing air and the building materials of the wall assembly. Therefore, in addition to the heat transfer behavior, analysis of the moisture accumulation (considering moisture sorption-retention curves of the materials) over time was needed. The CHAMPS-BES software was used to simulate the combined heat, air, and moisture transfer through the wall layers.

The model has been built on the Delphin 5 program.[14] The internal energy balance, air, and moisture mass balance are written as:

$$\frac{a\rho^U}{ax} = -\frac{a}{ax}(\mu j_{conv}^v + j_{diff}^Q + h j_{diff}^V) + \sigma_{ref}^U \qquad (4)$$

$$\frac{a\rho^{ma}}{ax} = -\frac{a}{ax} j_{conv}^{ma} + \sigma_{ref}^{ma} \qquad (5)$$

$$\frac{a\rho^{mw+v}}{ax} = -\frac{a}{ax}(j_{conv}^{mw} + j_{conv}^{mv} + j_{diff}^{mv}) + \sigma_{ref}^{mw+v} \qquad (6)$$

where

ρ^U = internal energy density, J/m³

μ = specific internal energy, J/kg

j_{conv}^v = convective water vapor flux, kg/(m²s)

j_{diff}^Q = heat conduction, J/(m²s)

h = specific of water vapor in J/kg

σ_{ref}^U = energy sources/sinks, J/m³s

$\rho^m{}_a$ = air mass density in reference volume, kg/m³

j_{conv}^{ma} = convective air mass flux, kg/(m²s)

σ_{ref}^{ma} = air sources/sinks in reference volume, kg/(m³s)

$\rho^m{}_{w+v}$ = moisture density, kg/m³

j_{conv}^{mw} = convective liquid (capillary) water flux, kg/(m²s)

j_{conv}^{mv} = convective water vapor flux, kg/(m²s)

j_{diff}^{mv} = diffusive water vapor flux, kg/(m²s)

σ_{ref}^{mw+v} = moisture sources/sinks in reference volume, kg/(m³s)

Figure 3 shows an overview of the modeling workflow. In this study, two different sections (a vertical section and a corner section) were analyzed. The three-dimensional (3-D) heat transfer problem for the corner was simplified and reduced to a 2-D problem. For the vertical section, two types of models—one without any leakage path (only energy balance), and one with leakage path (energy and air and moisture mass balances accompanied by interior and exterior air pressure boundaries)—were created. The actual leakage area ratio was calculated and was accounted for in the model geometry creation. Two difference leakage scenarios were considered: leakage path (a) was a symmetrical path and accounted for the leakage from the panel-to-panel seam interfaces, and leakage path (b) was unsymmetrical.

Steady-state and transient simulations were performed. Material properties and parameters were obtained from the built-in libraries of CHAMPS-BES. Additional material properties were set based on laboratory measurements for the graphite polystyrene and manufacturers' data sheets for the gasket materials.

For the steady-state simulations, both winter and summer conditions were analyzed. For the winter simulations, the indoor temperature was set to 21°C (69.8°F), and the indoor relative humidity (RH) was set to 25%. The outdoor temperature was assumed to be −16.7°C (62.06°F) (heating design condition for Syracuse), and the outdoor RH was assumed to be 80%. The initial temperature over the whole wall was 0°C (32°F), and the initial RH over the whole wall domain was 55%. For the summer simulations, the indoor temperature was set to 24°C (75.2°F),

and the indoor RH was set to 50%. The outdoor temperature was assumed to be 30°C (86°F) (cooling design condition for Syracuse), and the outdoor RH was assumed to be 70%. The initial temperature over the whole wall was 22°C (71.6°F), and the initial RH over the whole wall domain was 55% for the summer simulations.

For the transient condition, the actual measured values were used to determine the simulated average heat flux over the interior surface and compare it with the average measured heat flux. For the models with leakage paths, interior and exterior air pressure boundaries were added (5, 10, and 20 Pa pressure difference), and both exfiltration and infiltration conditions were analyzed.

The energy-saving potentials were estimated by computer simulations using Design Builder/EnergyPlus software.[11] Simulations were performed to determine the annual thermal energy consumption for before and after the whole-building retrofit solution was applied. The baseline condition before the retrofit represents the median thermal EUI of the single-family attached building type in US.

RESULTS AND DISCUSSION

The air gap temperature followed the trend of outdoor air temperature in most cases (indicating the presence of infiltration airflow) with a few exceptions in which the temperature in the air gap was similar to the indoor air temperature (indicating the presence of exfiltration airflow). The heat flux variation was shown in **Fig. 4** (left), which correlated well with the indoor-outdoor air temperature difference, and was not obviously affected by the air gap temperature. This may be
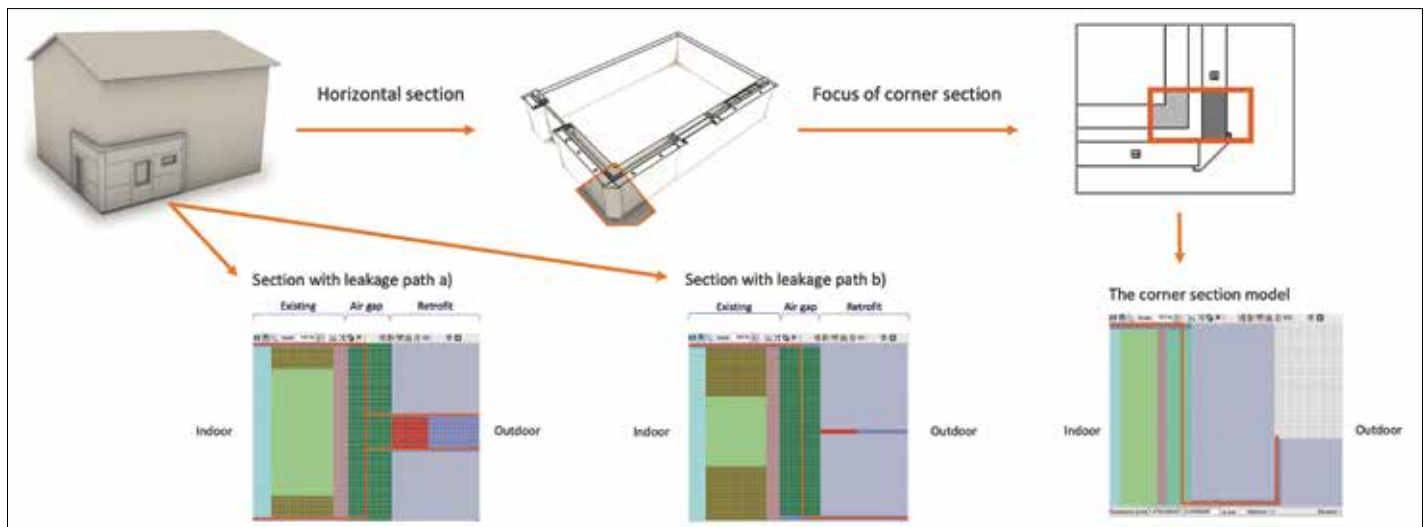

Figure 3. *Overview of the modeling workflow and CHAMPS-BES simulation setup.*
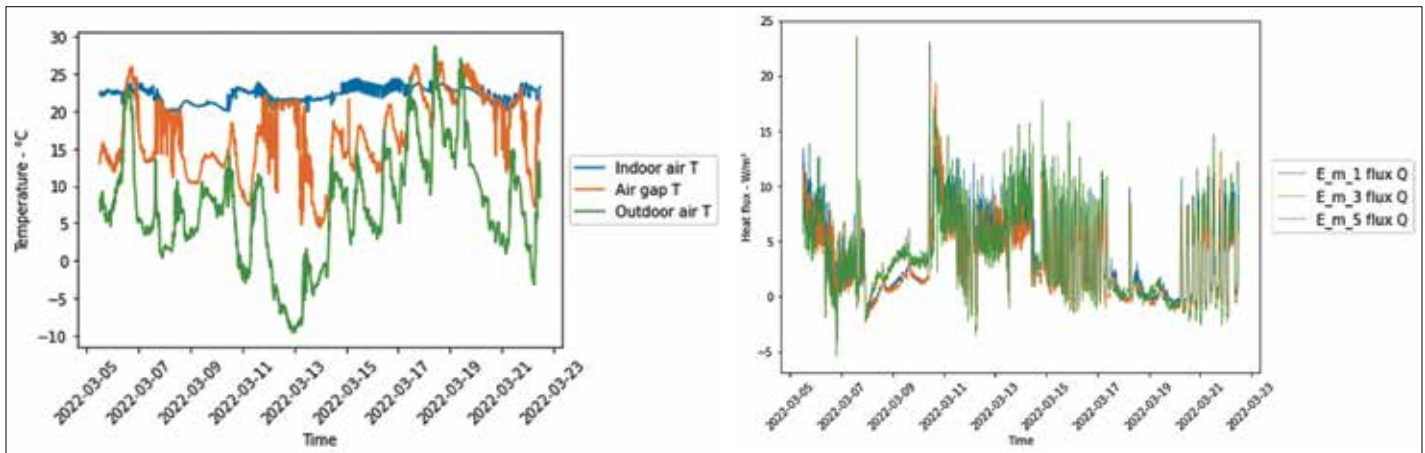
Figure 4. *Thermal conditions for sections 1, 3, and 5 of the east walls during the running period: indoor temperatures, temperatures in the air gap between the existing exterior wall and the retrofitting panel, and outdoor temperatures (left); heat fluxes (right).*

due to the thermal mass of the wall that made the heat flux less sensitive to the fluctuating air gap temperature due to infiltration/exfiltration. Even though section 1, 3, and 5 were at different locations, there were small differences among their monitored heat flux values. This indicated similar insulation performance of the opaque wall sections regardless of orientation and elevation.

Table 1 presents the coefficients of variance and standard deviations of *R*-values. The coefficients of variance were less than 10%; the mean *R*-values for the existing construction and the retrofitting panel were 1.59 and 2.53 m^2K/W (9.02 and 14.36 $ft^2 \cdot °F \cdot h/BTU$), respectively (71.6°F), with mean standard deviations of 0.04 and 0.18 m^2K/W (0.22 and 1.02 $ft^2 \cdot °F \cdot h/BTU$).

Figure 5 shows the temperature contours for the sections with leakage paths (a) and (b) for the three pressure-difference scenarios for the steady-state exfiltration and infiltration conditions. As can be seen from the comparison of the sections without and with leakage paths, the presence of an air leakage path significantly affected the contours. Because of the considered leakage paths,

TABLE 1. Coefficients of variance and standard deviations (SDs) for *R*-values

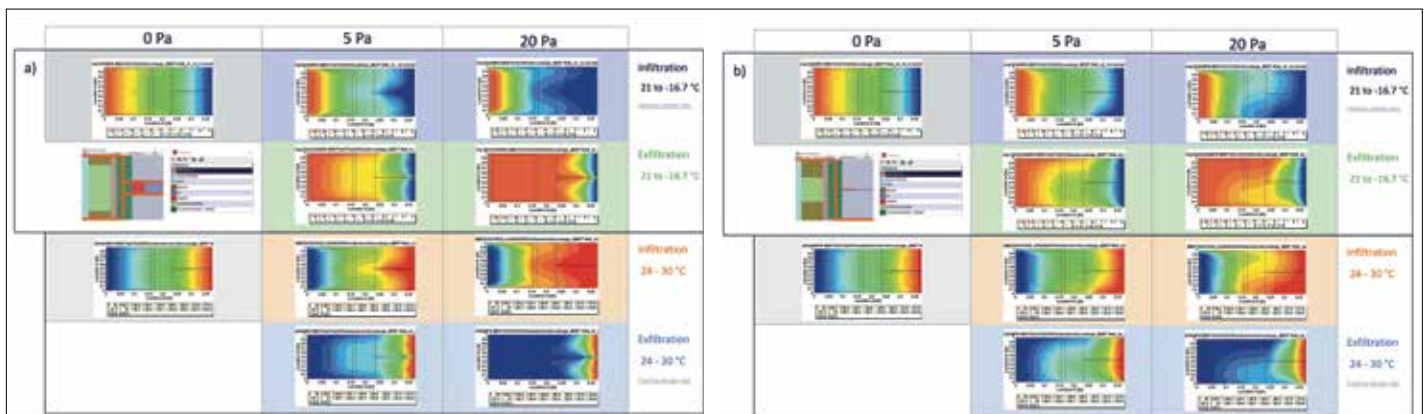| Wall sections	Existing construction			Retrofitting panel		
	R-value, m²K/W	Coefficient of variance	SD, m²K/W	*R*-value, m²K/W	Coefficient of variance	SD, m²K/W
E_m_1	1.53	3%	0.04	2.43	7%	0.16
E_m_3	1.76	2%	0.04	2.80	7%	0.21
E_m_5	1.48	2%	0.03	2.35	7%	0.17
Average	1.59	2%	0.04	2.53	7%	0.18

Figure 5. *Temperature contours for the sections with leakage paths (a) and (b).*
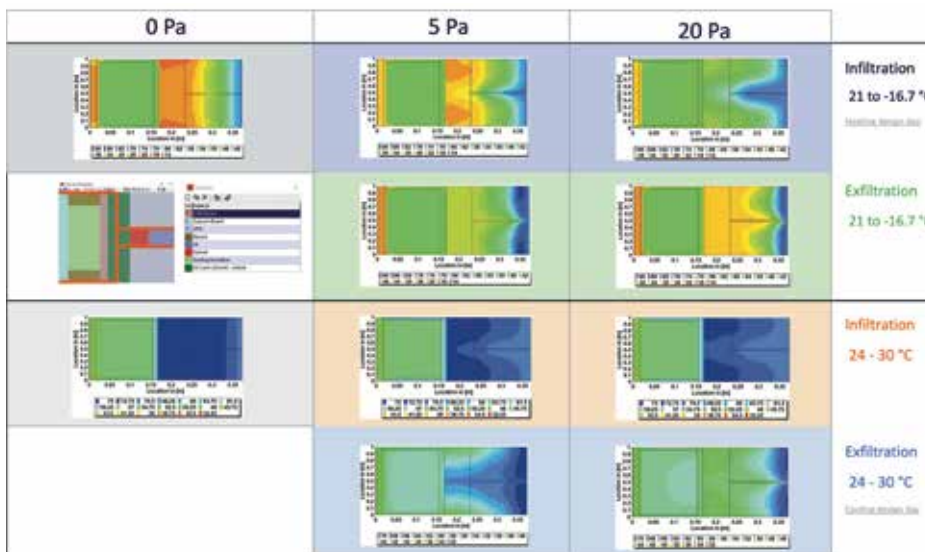
Figure 6. *Relative humidity distribution for the sections with leakage path (a).*

TABLE 2. Summary of simulation results for the sections with leakage paths (a) and (b)

Leakage path (a)				
		Pressure difference, Pa		
Parameter	**Location, mm**	**0**	**5**	**20**
Gypsum temperature, °C	0	20.4	19.66	18.65
Oriented strand board temperature, °C	168.275	5.1	−3.45	−11.11
Air cavity temperature, °C	200.275	3.74	−6.55	−13.91
Inside panel temperature, °C	232.275	3.82	−4.75	−12.52
Outside panel temperature, °C	371.975	−16.5	−16.62	−16.7
Gypsum heat flux, W/m^2	0	4.82	10.64	18.1
R-value for existing structure, m^{2}K/W		3.46	2.46	1.8
R-value for retrofit, m^{2}K/W		4.2	0.95	0.15

Leakage path (b)				
		Pressure difference, Pa		
Parameter	**Location, mm**	**0**	**5**	**20**
Gypsum temperature, °C	0	20.4	20.04	19.44
Oriented strand board temperature, °C	168.275	5.38	0.65	−7.2
Air cavity temperature, °C	200.275	4.6	0.02	−8.03
Inside panel temperature, °C	232.275	4.25	−0.75	−8.82
Outside panel temperature, °C	371.975	−16.5	−16.6	−16.65
Gypsum heat flux, W/m^2	0	4.72	7.65	12.5
R-value for existing structure, m^{2}K/W		3.35	2.62	2.2
R-value for retrofit, m^{2}K/W		4.47	2.17	0.69

results from the scenario known as leakage path (a) repres (71.6°F) ent more symmetric contours, and it was most severe for the 20 Pa pressure difference.

Figure 6 shows the simulated RH distributions for the sections with leakage path (a) for the three pressure-difference scenarios for exfiltration and infiltration conditions. These distributions are notable given the severity of the influence of air leakage on the wall's performance.

Table 2 summarizes the simulation results for the sections with leakage paths (a) and (b). It shows that leakage effects on thermal resistance increased from 13% to 35% as pressure difference increased from 5 to 20 Pa. **Figure 7** shows the temperature contours for the corner section for the 5- and 20-Pa pressure-difference infiltration conditions. The average interior heat fluxes for the 5- and 20-Pa cases were 13.87 and 20.58 W/m^2 (4.39 and 6.53 BTU/h·ft²), respectively.

Then, the transient conditions were analyzed using the interior heat-flux data for the first four days of March. **Figure 8** shows the comparison of simulated and measured data for the 0-, 5-, and 10-Pa pressure-difference scenarios for leakage paths (a) and (b). **Table 3** summarizes the error quantification results for these comparisons. Field measurement data on temperature and heat flux validated the simulation results, with average mean absolute error of 1.07 W/m^2 and root mean square error (RMSE) of 1.31W/m^2 (0.33 BTU/h·ft²). **Figure 9** provides a comparison of the wall liquid content with and without leakage. The leakage model results of moisture for both scenarios (a) and (b) for moisture provide an overview of the differences over the four-day analysis period.

Step wise energy simulations were performed to determine the incremental thermal energy savings due to each retrofit strategy in comparison with the median thermal EUI baseline building conditions. These results were presented as an evaluation of various components of the retrofit prototype, based on the measured input values, and their combined effect on the building enclosure performance and overall energy saving potential. However, they do not represent the results from the final retrofit solution. The final retrofit solution will be validated in the field. **Table 4** shows the impact of the enclosure and HVAC pod strategies, which provides 80.3% thermal energy saving
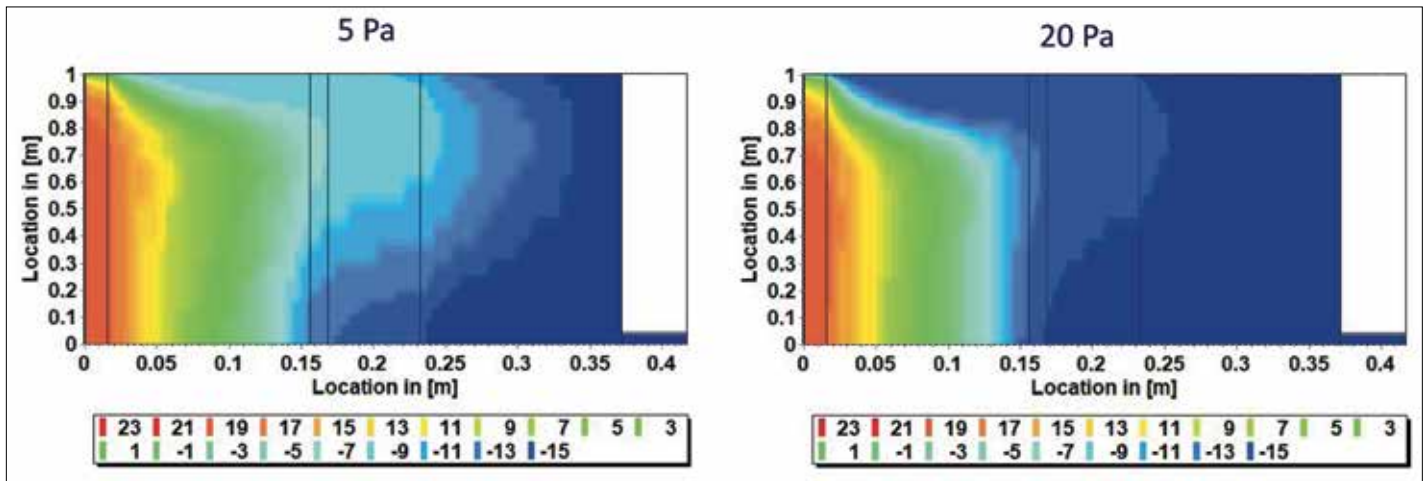
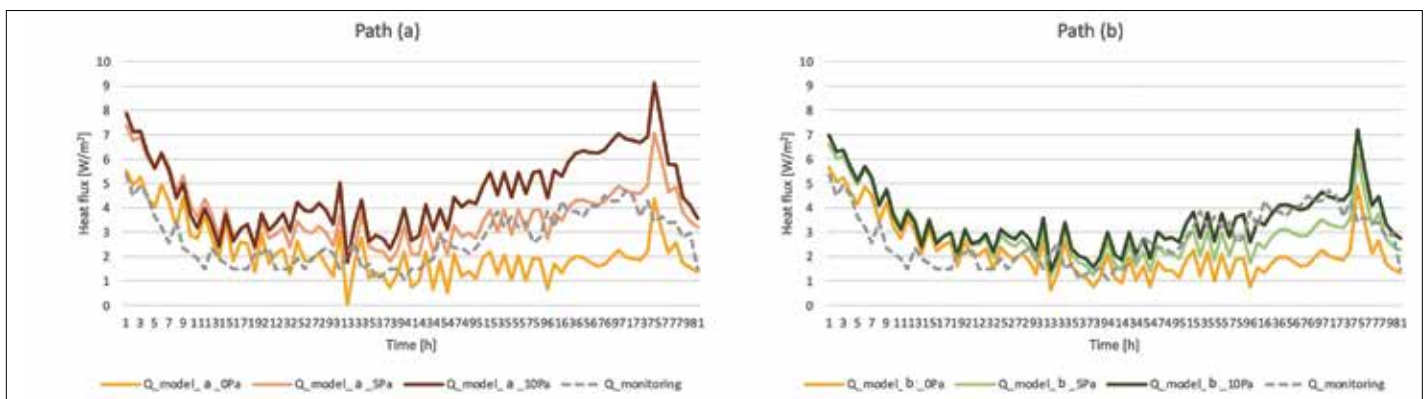**Figure 7.** *Temperature contours for the corner section.*

Figure 8. *Comparison of simulated and measured interior heat flux data of 0-, 5-, and 10-Pa pressure difference scenarios for leakage paths (a) and (b).*

TABLE 3. Summary of the error quantification results for the heat-flux comparisons

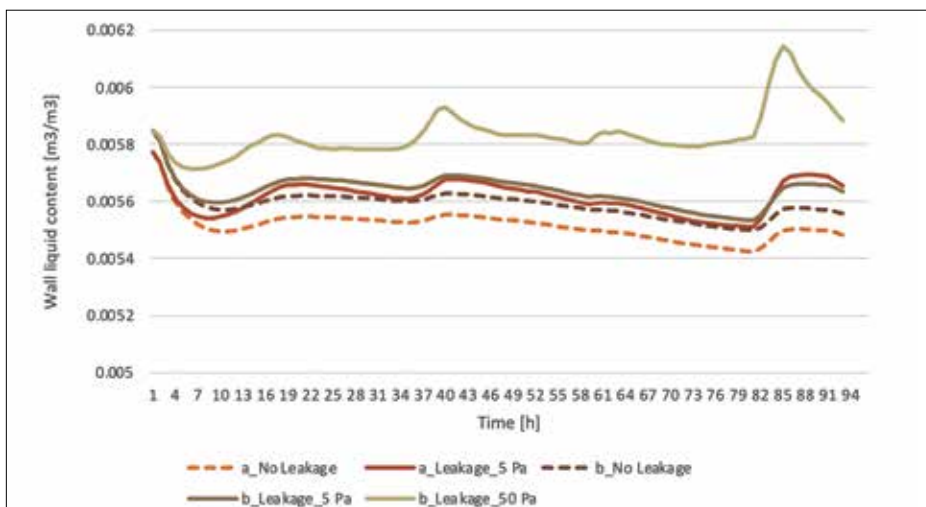|	Leakage path (a)			Leakage path (b)		
	0 Pa	5 Pa	10 Pa	0 Pa	5 Pa	10 Pa
MAE, W/m²	1.17	1.13	1.13	1.14	0.93	0.92
RMSE, W/m²	1.42	1.39	1.39	1.39	1.16	1.16

Figure 9. *Comparison of the wall liquid content with and without leakage.*

after the retrofit. Improving the airtightness to 2.14 ACH50 leads to 0.3% reduction in thermal EUI. Then, adding the retrofit panel resulted in 8% reduction of the building's thermal EUI comparing to the baseline. A subtotal of 8.3% thermal EUI reduction was achieved by retrofitting the enclosure. It also shows the incremental thermal EUI reductions due to increased equipment efficiency for air heating (43%), cooling (0.5%) and domestic water heating (28.5%), with a subtotal thermal EUI reduction of 72% from the energy pod. From the total thermal EUI reduction (80.3%) from the integrated retrofit solution, 44.92% was from space heating, 0.70% from space cooling, 6.11% from ventilation, and 28.56% from the water heating energy reductions. It should be noted that the calculated *R*-value is lower than the target value and the airtightness level is higher than the goal. The *R*-value for the retrofitting panel includes leakage and joint effects, and the analysis showed that 33% thermal leaks took place at the top and bottom boundaries of the retrofitting assembly due to insufficient insulation and

TABLE 4. Specific energy-savings for median thermal EUI single-family attached residences

Retrofit strategy	Baseline[a]	Project goal	Achievable in Prototype	Specific strategies	Incremental annual energy savings	Energy savings subtotal
Airtightness	2.2 ACH_{50}[b]	1.05 ACH_{50}	2.14 ACH_{50}	Precompressed foam tape gasket solution, enclosure, integrated window and door installation	0.3%	8.3%
Insulation	*R*-value of 17[d]	*R*-value of 30 (measured *R*-value = 27[e])	*R*-value of 16.97[g]	Insulated prefabricated panel solution, including panelized roof modules	8%	
Heating equipment efficiency	80 AFUE[d]	3.0 COP	4.24 COP	Pod-based heat pumps	43%	72%
Cooling equipment efficiency	9.1 EER[d]	23 EER	23 EER	Pod-based heat pumps	0.5%	
Domestic Hot Water (DHW) efficiency	0.56 EF[d]	2.43 EF	2.43 EF	Pod-based heat pumps	28.5%	
Expected energy savings	–	75%		–	–	80.3%
Indoor air quality		<800 ppm of CO_2		Pod-based energy recovery ventilation with heat- recovery efficiency of at least 80% and CO_2-enabled boost function		

a   Baseline conditions for single-family attached building located at 150 Small Road, Syracuse, N.Y.

b   Estimated airtightness level for single-family attached buildings in cold climate regions.

c   Based on the target airtightness of maximum 1.0 L/s/m² exterior enclosure surface area at 50 Pa.

d   2014 Building America House Simulation Protocols by the National Renewable Energy Laboratory for buildings built between 1980 and 1989.

e   Based on the midscale Building Energy and Environmental Systems Laboratory's chamber test results for retrofitting panels. (R-value of 27 was used as additional insulation from the panel.)

f   Elimination of the top- and bottom-joint effects, which occupied 30% of the total joints by leakage area (total measured air leakage rate was 3.19 ACH50).

g   Effective R-value for the retrofitting panel, ignoring the top- and bottom-joint effects.

sealing. As mentioned before, the reported results are based on the project prototype, but the final solution will be validated in the field. If the main issues are corrected, based on the project goal (values reported on the Project Goals column), 78% thermal energy is saved after the retrofit (savings of 14.4% from the enclosure system and 63.6% from the integrated HVAC pod).

CONCLUSION

This case study explored the significant potential of prefabricated, panelized exterior insulated enclosure systems for retrofitting single-family attached residences in cold climates. By integrating numerical tools with in situ measurements, the performance of a full-scale, integrated energy efficiency retrofit assembly was thoroughly evaluated. The research specifically focused on the impact of air leakage on hygrothermal behavior of the exterior insulated envelope systems. The effect of air leakage on hygrothermal behavior, especially moisture, was shown to be significant. CHAMPS-BES software enabled the testing of integrated retrofit walls compared with actual field testing, providing a cost-effective way to predict assembly behavior. However, the airflow model (combining heat, air, and moisture transfer) required significantly more computational time than was needed for the actual hygrothermal wall model (design without leakage). Although simulations of air leakage are more accurate, they are computationally complex and not typically considered for design and evaluation. The energy model developed and applied for Syracuse, New York, estimated an impressive 80.3% reduction in thermal EUI through a retrofitting approach that included an exterior insulated panel system combined with enhanced mechanical equipment efficiency. The numerical modeling, simulation, and measurements not only facilitated practical suggestions for strengthening building enclosure panel elements and evaluating retrofit solutions but also laid the foundation for methodological advancements in the design, construction, operation, and retrofitting of energy-efficient buildings.

ACKNOWLEDGMENTS

REFERENCES

1. IEA. Towards a Zero-Emission, Efficient and Resilient Buildings and Construction Sector. (2018).

2. USCB (U.S. Census Bureau). American FactFinder: Selected Housing Characteristics. https://factfinder.census.gov/faces/tableservices/jsf/pages/productview. xhtml?pid=ACS_17_5YR _DP04&src=pt (2017).

3. Mata, E., Kalagasidis, A. S. & Johnsson, F. Contributions of building retrofitting in five member states to EU targets for energy savings. Renewable and Sustainable Energy Reviews vol. 93 759–774 Preprint at https://doi.org/10.1016/j. rser.2018.05.014 (2018).

4. Webster, B. et al. Accelerating Residential Building Decarbonization: Market Guidance to Scale Zero- Carbon-Aligned Buildings. (2024).

5. Mirzabeigi, S. & Razkenari, M. Multiple benefits through residential building energy retrofit and thermal resilient design. in 2022 (6th) Residential Building Design & Construction Conference 456–465 (University Park, 2022).

6. Antonopoulos, C. A. et al. Wall Upgrades for Residential Deep Energy Retrofits: A Literature Review. https://www.ntis.gov/about (2019).

7. Kamel, E. & Memari, A. M. Residential Building Envelope Energy Retrofit Methods, Simulation Tools, and Example Projects: A Review of the Literature. Buildings vol. 12 Preprint at https://doi.org/10.3390/ buildings12070954 (2022).

8. Madushika, U. G. D., Ramachandra, T., Karunasena, G. & Udakara, P. A. D. S. Energy Retrofitting Technologies of Buildings: A Review-Based Assessment. Energies vol. 16 Preprint at https://doi.org/10.3390/ en16134924 (2023).

9. Mirzabeigi, S., Zhang, J. & Razkenari, M. Exterior Retrofitting Systems for Energy Conservation and Efficiency in Cold Climates: A Systematic Review. in Environmental Science and Engineering 413–422 (Springer Science and Business Media Deutschland GmbH, 2023). doi:10.1007/978-981-19-9822-5_44.

10. Nicolai, A., Grunewald, J. & Zhang, J. J. Recent improvements in HAM simulation tools: Delphin 5/CHAMPS-BES. in 12th International Building Physics Conference (Dresden, Germany, 2007).

11. Crawley, D. B., Lawrie, L. K., Winkelmann, F. C. & Pedersen, C. O. EnergyPlus: A New-Generation Building Energy Simulation Program. in Forum 2001: Solar Energy: The Power to Choose (2001).

12. Mirzabeigi, S., Zhang, R., Krietemeyer, B. & Zhang, J. "Jensen". Modeling the Effects of Panel Interfaces on Airtightness and Thermal Performance of an Integrated Whole-Building Energy Efficiency Retrofit Assembly. in International Buildings Physics Conference 2024 (2024).

13. ASTM. C1155-95—Standard Practice for Determining Thermal Resistance of Building Envelope Components from the In-Situ Data. www.astm.org, (2021) doi:10.1520/C1155-95R21.

14. Langmans, J., Nicolai, A., Klein, R. & Roels, S. A quasi-steady state implementation of air convection in a transient heat and moisture building component model. Build Environ 58, 208–218 (2012).

ABOUT THE AUTHORS

SHAYAN MIRZABEIGI

Shayan Mirzabeigi, *LEED Green Associate, is a PhD candidate in sustainable construction management at the State University of New York College of Environmental Science and Forestry. He is also pursuing a second PhD in mechanical engineering at Syracuse University. He received his bachelor's degree from the University of Tehran and an MS in building engineering from Politecnico di Milano. Mirzabeigi has worked on several independent and collaborative research projects related to building energy performance, building enclosure systems, and computer vision.*

SAMEERAA SOLTANIAN-ZADEH

Sameeraa Soltanian-Zadeh *is a PhD student in mechanical and aerospace engineering at Syracuse University. She has a bachelor's degree in architectural engineering from the University of Tehran and a master's degree in building engineering from Politecnico di Milano. She is a recipient of the US Department of Energy 2024 IBUILD Fellowship. Her research focuses on indoor air quality and urban environmental dynamics, highlighting the impact of occupant behaviors impact on indoor air quality and building energy efficiency. By examining diverse building types across different communities and income levels, her research contributes to environmental justice, offering insights for public health, energy efficiency, and sustainable urban development, especially regarding the role of building occupants.*

RUI ZHANG, PHD

Rui Zhang, *PhD, works as a postdoctoral research associate in the Transportation Science and Buildings Division at Oak Ridge National Laboratory. Zhang earned a master's degree and PhD in mechanical engineering from Syracuse University, where she focused on modeling computational fluid dynamics, indoor air quality, and building energy consumption during her master's studies, and studied the impact of atmospheric corrosion on computer technology in data centers for her doctorate. Zhang's current research focuses on energy-efficient retrofit solutions for residential buildings, bio-based building materials, and building air leakage and moisture detectors. She also develops bio-based vacuum insulation panels.*

ZHENLEI LIU, PHD

Zhenlei Liu, *PhD, works in the Transportation Science and Buildings Division at Oak Ridge National Laboratory as a postdoctoral research associate. He earned his PhD in mechanical engineering from Syracuse University, where he conducted pioneering research on building energy efficiency and indoor air quality. His work included examining the transmission and control of diseases like COVID-19 in indoor spaces, developing models to simulate Volatile Organic Compounds (VOC) emissions under various indoor environmental conditions using a model-based testing method, and exploring the use of Metal Organic Frameworks (MOFs) in building and HVAC equipment. He currently leads and participates in research on non-energy*

impacts for energy audits, measurement and verification (M&V) with cutting-edge technologies, and cost-effectiveness analysis with predicted future weather as part of the DOE's Weatherization Assistance Program.

BESS KRIETEMEYER, PHD

Bess Krietemeyer, *PhD, is an associate professor at the Syracuse University School of Architecture. She has experience in architectural design, deep energy retrofits, decision analysis tools, and academic-industry partnerships. Her research has been supported by the US Department of Energy (DOE), the National Science Foundation, and the New York State Energy Research and Development Authority (NYSERDA). Her current work includes leading a DOE Advanced Building Construction project to develop a holistic deep energy retrofit for low- to moderate-income residences in cold climates. Additionally, she* is working on projects through the DOE EPIC program that focus on equity and health in grid-interactive and energy-efficient buildings, the National Renewable Energy Laboratory Building America Program, and the NYSERDA Energy to Lead program focused on the energy and health benefits of deep energy retrofits.

JIANSHUN "JENSEN" ZHANG, PHD

Jianshun "Jensen" Zhang, *PhD, is a professor of mechanical and aerospace engineering and the executive director of the Syracuse Center of Excellence in Environmental and Energy Systems at Syracuse University. He has over 30 years* of research and teaching experience in built environmental systems. His research ranges from multiscale building environmental systems from nano/micro-scale in porous materials to buildings and urban environment, involving engineering, architectural design, and health and human performance. He served as a US expert for several International Energy Agency projects (IEA-EBC Annex 20, 68, 78, 86 and 92) in building energy efficiency and indoor air quality, and he served as president of International Association of Building Physics (2018–2021). Zhang is a fellow of ASHRAE and the International Society of Indoor Air Quality and Climate. The author of more than 200 publications, he is the current editor-in-chief of the International Journal of Ventilation *and* associate editor of Science and Technology for the Built Environment.

Please address reader comments to chamaker@iibec.org, including "Letter to Editor" in the subject line, or IIBEC, *IIBEC Interface* Journal, 434 Fayetteville St., Suite 2400, Raleigh, NC 27601